Frontiers | Frontiers in Environmental Science

TYPE Original Research
PUBLISHED 27 November 2025
DOI 10.3389/fenvs.2025.1684687

Check for updates

OPEN ACCESS

EDITED BY
Željka Fiket,
Rudjer Boskovic Institute, Croatia

REVIEWED BY
Meng Chuan Ong,
University of Malaysia Terengganu, Malaysia
Renata Mascarenhas,
Federal University of Bahia (UFBA), Brazil

*CORRESPONDENCE
Rafael Tarantino Amarante,
✉ rafaeltageo@gmail.com,
✉ rafael.amarante@pq.itv.org

RECEIVED 12 August 2025
REVISED 03 November 2025
ACCEPTED 10 November 2025
PUBLISHED 27 November 2025

CITATION
Amarante RT, Marques ED, Ruchkys ÚA, Silva-Filho EV, Almeida GS, Mello I and Salomão GN (2025) Geochemical baseline and multivariate analysis of potentially toxic elements in stream sediments of the Vazante zinc district, Minas Gerais, Brazil.
*Front. Environ. Sci.* 13:1684687.
doi: 10.3389/fenvs.2025.1684687

# Geochemical baseline and multivariate analysis of potentially toxic elements in stream sediments of the Vazante zinc district, Minas Gerais, Brazil

Rafael Tarantino Amarante[1,2,3]*, Eduardo Duarte Marques[3,4], Úrsula Azevedo Ruchkys[1], Emmanoel Vieira Silva-Filho[3], Gabriel Soares Almeida[2], Isadora Mello[3] and Gabriel Negreiros Salomão[2]

[1]Programa de Pós-Graduação em Análise e Modelagem de Sistemas Ambientais, Instituto de Geociências, Universidade Federal de Minas Gerais, Belo Horizonte, Minas Gerais, Brazil, [2]Instituto Tecnológico Vale, Belém, Pará, Brazil, [3]Programa de Pós-Graduação em Geociências (Geoquímica), Instituto de Química, Universidade Federal Fluminense, Rio de Janeiro, Brazil, [4]Serviço Geológico do Brasil, SGB/CPRM, Superintendência de Belo Horizonte, Belo Horizonte, Minas Gerais, Brazil

Intense land use, driven by mining and agriculture, promotes the dispersal of elements, including potentially toxic ones (PTEs). This dispersal significantly enhances element concentrations in soils, sediments, and water bodies, thereby altering the natural background values of the environment. The objective of this paper is to employ geochemical mapping alongside multivariate statistical methods to establish the baseline values for the Mining Zinc District situated at the boundary of the São Francisco Craton and Brasília Belt. This will facilitate the assessment of spatial variability and determination of reference values for element concentrations in sediment samples, enabling the differentiation between natural and anthropogenic sources of potentially toxic elements. A geochemical database of 1853 sediment samples were assembled from the São Francisco and Paranaíba watersheds for subsequent ICP-OES and ICP-MS analysis. The baseline values were assessed through 3 distinct methods, while the Factor Analysis was employed as a multivariate statistical technique. The findings reveal that the baseline concentrations of Ni (415 $mg.kg^{-1}$), Cr (137 $mg.kg^{-1}$), and Co (106 $mg.kg^{-1}$) were higher than the Investigation Values of CONAMA Resolution n°454/2012. The factor analysis found 6 main factors that explain 75.1% of the total system variance. It also found 8 major geochemical links between these factors: (1) Al, Cs, Ga, Sn, and V; (2) Co, Mg, Ni, and Zn; (3) Cr, Ni, and V; (4) Cs, K, and Rb; (5) As, and Fe; (6) Cd, Pb, and Zn; (7) LREE, Th, and U; and (8) Ba, P, and Sr.

KEYWORDS

**geochemical mapping, baseline, sediments, multivariate analysis, São Francisco Craton**

# 1 Introduction

The Vazante Zinc District is a region of complex geological substratum and economic importance (Almeida, 1981; Dardenne et al., 1997; Dardenne, 2000). Its geology is marked by a world-class hypogene zinc silicate deposit, significant sedimentary phosphate resources (Rocinha and Lagamar), and occurrences of high potassium-rich “verdete” rocks (Dardenne, 2000; Monteiro, 2002; Moreira, 2015). The area also hosts over 200 kimberlite/lamproite bodies and the prominent Serra Negra ultramafic alkaline intrusion, which exhibits $TiO_2$ content as high as 34% (Pereira and Fuck, 2005; Pinho et al., 2017). Despite the rich geological context and economy driven by mineral resources, this region has considerable expansion of agricultural business, which constitutes 16.2% of total production and contributes over 4% to the gross domestic product of Minas Gerais state (João Pinheiro, 2019). All those features make this region an important economic pole of Minas Gerais State and, by extension, the Brazilian economy.

The confluence of intensive land use and complex geology creates a significant environmental challenge. These activities primarily affect the environment by dispersing elements, particularly potentially toxic elements, which increase concentrations in soils, sediments, surface water, and groundwater, thereby changing the natural values of the environment (Almeida et al., 2024; Dellamatrice and Monteiro, 2014; Felix et al., 2007; Medeiros Filho et al., 2025; Ribeiro et al., 2007). Consequently, comprehending the geochemical baseline of a specific region is essential for elucidating the geochemical processes that affect land management, especially in areas with significant anthropogenic influence (Almeida et al., 2024; Buccianti et al., 2008; Carranza, 2011; Cheng, 2007; Medeiros Filho et al., 2025; Meloni et al., 2025; Niu et al., 2024; Thornton et al., 2008).

Previous geochemical baseline and background studies typically treat a geologically diverse region as a single unit (Albanese et al., 2007; Meloni et al., 2025; Niu et al., 2024; Salomão et al., 2021; de Vicq et al., 2015), while these works provide valuable geological context, they often lack the detailed, multi-element approach and the robust statistical analysis required to establish a comprehensive geochemical baseline. Also, Brazilian legislation such as CONAMA resolutions 420/2019 (Brasil, 2009), propose that each state define their own Quality Reference Values (QRVs), but they are often defined broadly for an entire state. They do not account for the specific geological and geochemical characteristics of each region, particularly those within a metallogenetic province. The state of Minas Gerais has a vast geological diversity and hosts different mineral deposits. In such environments, the natural concentrations of elements like iron, manganese, chromium, nickel, and cobalt can be naturally elevated due to background geology.

Using a single reference value for the entire state, without considering parental geology, could lead to a misinterpretation, classifying naturally enriched areas as contaminated. A single, area-wide baseline is insufficient in such a setting, as it fails to account for the natural geochemical variability imposed by the distinct underlying lithologies. Specifically, a dedicated study aimed at systematically differentiating the complex geogenic signatures from emerging anthropogenic inputs in the stream sediments of the Vazante District has not yet been undertaken. This knowledge gap, particularly the absence of lithology-controlled baseline values, hinders the development of locally adapted environmental quality standards and effective land management strategies.

To address this challenge, this study employs a methodology that refines the traditional approach by integrating geochemical mapping with two critical components: the application of multivariate statistical analysis and the establishment of lithology-specific baselines. While traditional univariate maps display the distribution of single elements, multivariate techniques like factor analysis can process large, complex datasets to reduce dimensionality and reveal underlying geochemical processes (Albanese et al., 2007; Çavdar et al., 2025; Darnley, 1995; Darnley and Garrett, 1990; Eduardo et al., 2023; Gałuszka, 2007; Jean-Lavenir et al., 2025; Sahoo et al., 2020; Sahoo et al., 2020; Silva-Filho et al., 2014). This approach is crucial for identifying elemental associations and recognizing distinct geochemical patterns from natural, anthropogenic, or mixed sources, which are often undetectable through conventional interpretation (Boente et al., 2018; Buccianti and Grunsky, 2014; Caritat et al., 2018; Liu et al., 2016; Petrik et al., 2017; Talebi et al., 2018).

The establishment of a geochemical baseline of elements has brought attention to their applicability and importance across multiple fields of knowledge, ranging from geological research for mineral exploration and as a guide for those creating environmental policies. Geochemical baseline studies were intensified in the last decades due to a global environmental awareness enhancement and the reinforcement of sustainable principles (Albanese et al., 2007; Almeida et al., 2024; Meloni et al., 2025; Niu et al., 2024; Salomão et al., 2019; 2021; de Vicq et al., 2015). Therefore, the primary objectives of this study are: (1) determine the distribution and behavior of Al, As, Au, B, Ba, Be, Bi, Ca, Cd, Ce, Co, Cr, Cs, Cu Fe, Ga, Ge, Hf, Hg, In, K, La, Li, ∑LREE, Mg, Mn, Mo, Na, Nb, Ni, P, Pb, Rb, Re, S, Sb, Sc, Se, Sn, Sr, Ta, Te, Th, Ti, U, V, W, Y, Zn and Zr in stream sediments of Vazante zinc disctrict using geochemical mapping; (2) employ multivariate analysis to identify the main geochemical associations; (3) establish lithology-specific geochemical baseline ranges for a suite of elements in stream sediments of the study area. This will provide an extensive understanding of the main geological and geochemical processes within a relevant mineral province.

# 2 Study area

The Vazante Belt is a structure situated at de southern border of the Brasília Belt, within the context of a collisional Neoproterozoic orogeny located at the western border of the São Francisco Craton (Almeida, 1981; Dardenne et al., 1997; Dardenne, 2000) (Figure 1). This region possesses a notable geotectonic context due to its rich lithological and structural geology (Figure 2). The Vazante Zinc District has a world-class hypogene zinc silicate deposit hosted in dolomitic rocks (Monteiro, 2002). Also, the Rocinha (415 Mt resource, 10%–15% $P_2O_5$) and Lagamar (5 Mt resource, 30%–35% $P_2O_5$) sedimentary phosphate deposits (fluorapatite) in the Serra de Santa Helena Formation (Bambuí Group) are also worth noteworthy (Dardenne, 2000; Slezak et al., 2013).

The study area is composed by 6 main lithological unities: (a) Araxá Group, (b) remobilized bedrock); (b) the Outer Zone of the

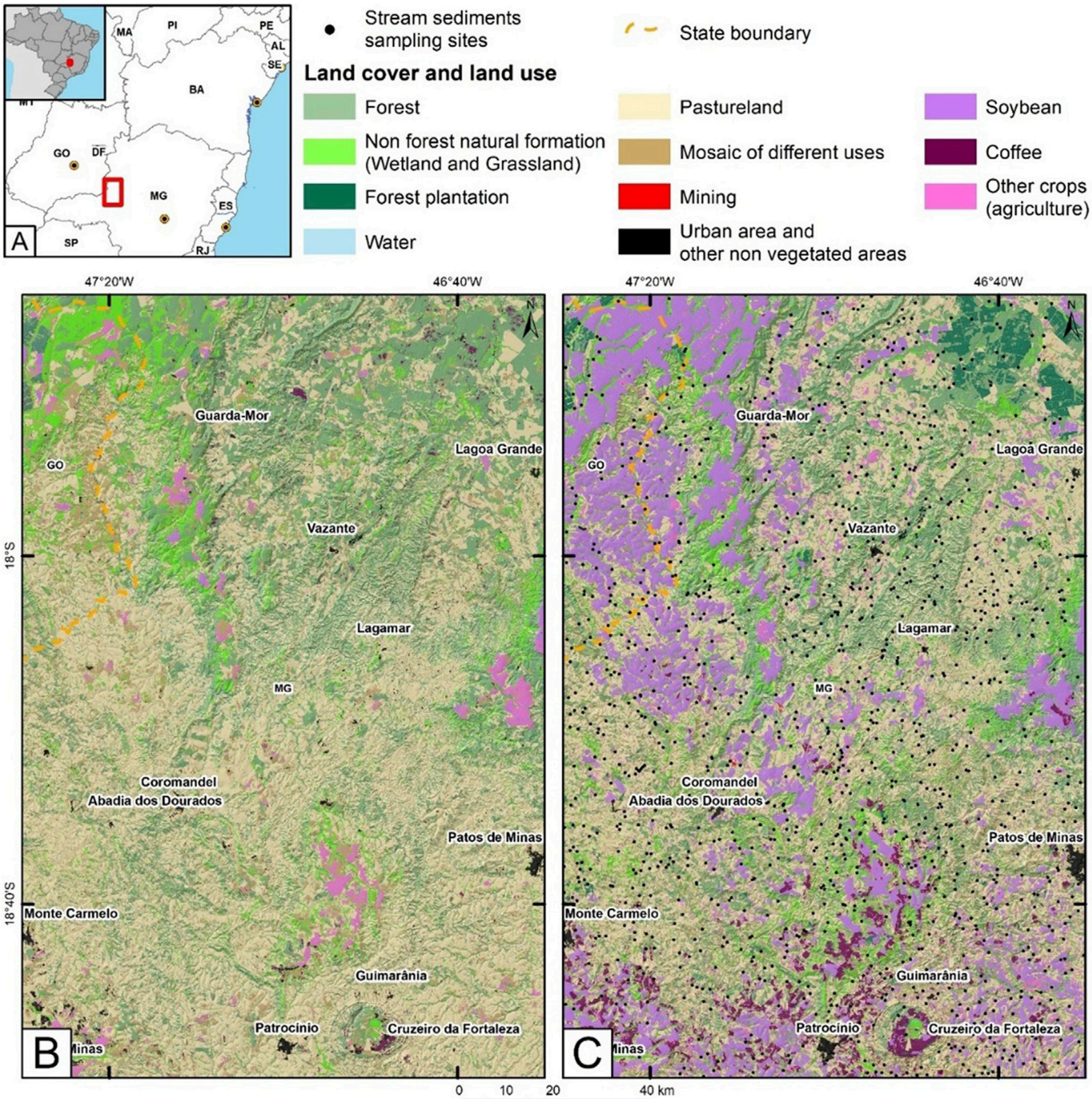

FIGURE 1
Location map of the study area **(A)**, overlaid by the land cover and land use classes in 1985 **(B)** and 2017 **(C)**. Source: (Souza et al., 2020).

Brasília Belt (Canastra and Ibiá groups); and (c) the São Francisco Craton Zone (Bambuí and Vazante groups) (Uhlein et al., 2012). The allochthonous unit of the Araxá Group consists of gneisses, mica schists, quartzites, and green schists, exhibiting features of ophiolitic mélange, including serpentinites and podiform chromite lenses derived from oceanic crust and upper mantle. The tectonic nappes of metasedimentary rocks on top of the amphibolite facies of the Araxá Group show that inverted metamorphism has happened in the IZ zone. These are subsequently located over the Bambuí Group, which exhibits a low degree of metamorphism (Caby et al., 1991; Uhlein et al., 2012). The Canastra Group consists of carbonaceous phyllites, quartzites and phyllites/schists occasionally severely deformed and exhibits metamorphism up to green schist facies. In contrast the Ibiá Group is composed of metadiamictites and schists (Dias et al., 2018; Uhlein et al., 2012).

The Bambuí Group exhibit amphibolite facies and are partially influenced by Neoproterozoic formation (Dias et al., 2018; Uhlein et al., 2012), also this unit presents small occurrences of “verdete” (high potassic content rocks), which reach about 9.65% of $K_2O$ (Moreira, 2015). There are also more than 200 kimberlites and lamproites bodies in the southern and southwestern parts of the area. These are mostly hosted by the Ibiá and Canastra groups, and the Serra Negra (ultramafic alkaline intrusion) with $TiO_2$ levels of about 34% (Pinho et al., 2017).

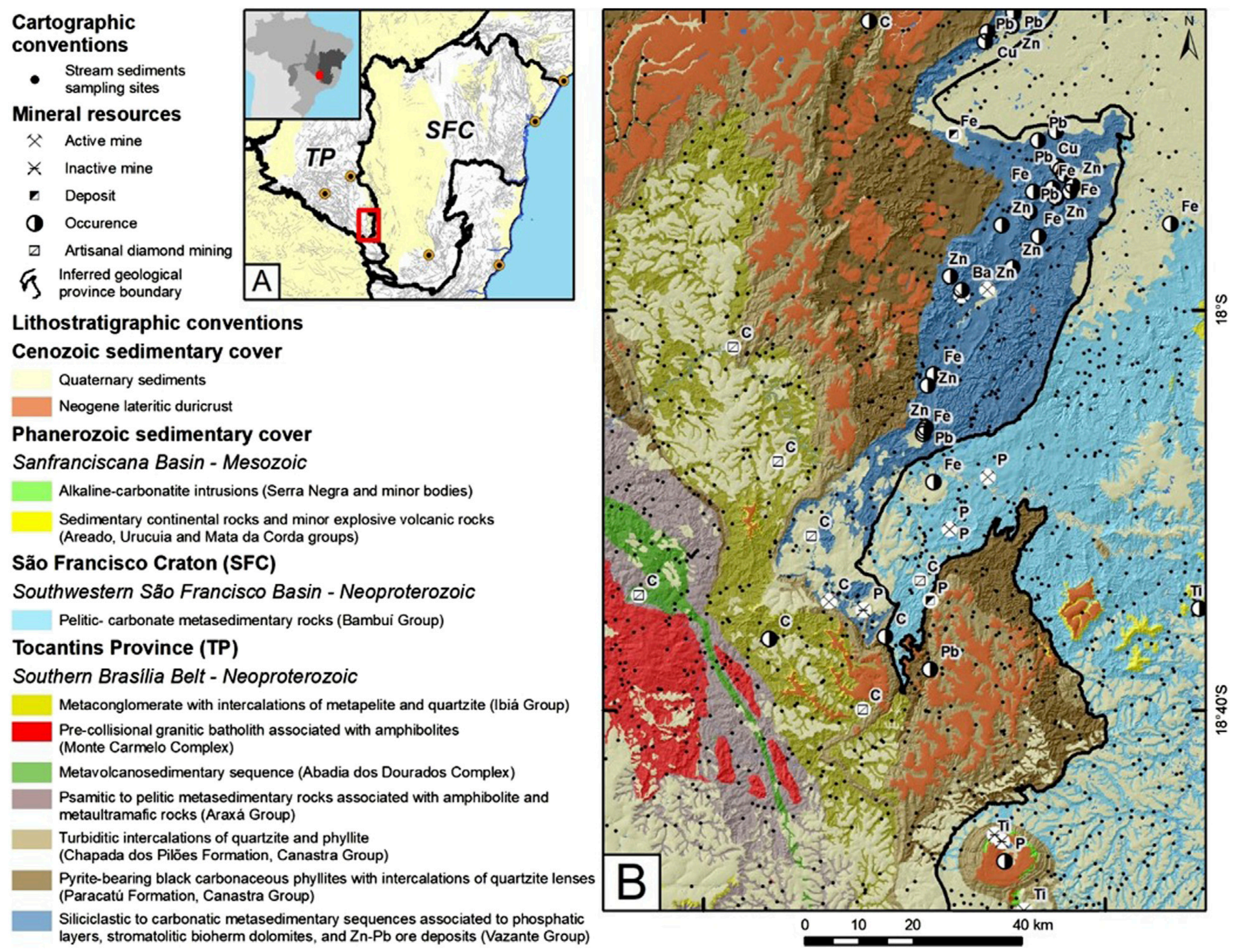

FIGURE 2
Geotectonically location **(A)** and geological map **(B)** of the study area. Source: (Silva et al., 2020).

# 3 Materials and methods

## 3.1 Geochemical dataset, sampling, and analytical methods

As a first methodological step, 1,835 samples of bottom sediment were collected from active stream channels by accredited laboratory SGS Geosol® and the Geological Survey of Brazil (SGB/CPRM) as part of the project Geologia e Recursos Minerais das Folhas: Cabeceira Grande, Unaí, Ribeirão Arrojado, Serra da Aldeia, Serra da Tiririca, Paracatu, Guarda-Mor, Arrenegado, Coromandel, Lagamar, Monte Carmelo e Patos de Minas (Pinho et al., 2017). All sample collection, preservation, packaging and analysis protocols were carried out based on the standards published in the 23rd edition of the Standard Methods for Examination of Water and Wastewater of the American Public Health Association (APHA - American Public Health Association, 2017).

Sediment samples were collected as a composite, consisting of 5–10 portions taken along a 50 m rectilinear transect and at a maximum depth of 1 m of the stream channel. All samples were collected with non-metal tools and pre-sieved using a 2 mm nylon strainer. After collection the samples were placed into transparent, and unprinted polyethylene plastic bags. Each bag was then sealed and clearly labeled with a unique identification code. The samples were placed in insulated containers with ice to maintain a temperature of approximately 4 °C and then were transported to the laboratory within the required holding time. The sediment samples were dried at 60 °C and sieved through 80 mesh (<0.175 mm) aperture sieves to access the granulometric range between fine-grained weathering products and coarse-fine fraction minerals as the elemental concentration within the silt and clay fractions of the sediment (Marques et al., 2023; Garrett, 2019; Rose et al., 1979).

For elemental determination, a 0.5 g aliquot of the pulverized material was subjected to a “pseudo-total” digestion with 3 mL of aqua regia (prepared in a 3:1 ratio of concentrated HCl to $HNO_3$). Following digestion, the extracts were diluted to a final volume of 10 mL with deionized water, and filtered for analysis via ICP-OES for major elements and ICP-MS for trace elements (Pinho et al., 2017). The use of two different spectrometric techniques is based on the distinct concentration ranges and characteristics of the target elements. Therefore, the combined use of ICP-OES and ICP-MS is not redundant but rather a strategic approach to optimize accuracy, working range, and cost-effectiveness, ensuring reliable results for both major and trace elements. A total of 50 chemical elements has been analyzed such as: Al, As, Au, B, Ba, Be, Bi, Ca, Cd, Ce, Co, Cr, Cs, Cu Fe, Ga, Ge, Hf, Hg, In, K, La, Li, ∑LREE, Mg, Mn, Mo, Na, Nb, Ni, P, Pb, Rb, Re, S, Sb, Sc, Se, Sn, Sr, Ta, Te, Th, Ti, U, V, W, Y, Zn and Zr.

The stream sediment samples were used to represent the average geochemical composition of all scattered material uphill of the sample collection site and to elucidate the main sources influencing the variety of components within the samples (Darnley, 1995). The accuracy and precision of the analytical procedure were validated through the analysis of replicates of the Certified Reference Material (CRM) OREAS 046 and 047, from ORE RESEARCH & EXPLORATION P/L. Each batch included three control samples: duplicates, replicates, and standard reference materials (SRMs). To investigate elemental variability, about 50 duplicate samples were collected from different locations. These duplicates were then subsampled to create replicated analytical samples, allowing them to assess the variations within both the sampling site and the individual sample. Also, blank samples were used to identify and measure any contamination that may be introduced during the analytical process, from sample collection to laboratory analysis.

## 3.2 Statistical analysis

The geochemical dataset was preprocessed utilizing Statistica (StatSoft), Microsoft Excel, and CoDaPack (Comas and Thio-Henestrosa, 2011). Robust statistics were applied including univariate and multivariate techniques to reduce dimension, identify major geochemistry trends, and investigate the natural sources of contamination and probable human influence on extreme concentrations of potentially toxic elements in the riverine environment (Grunsky, 2010; Reimann et al., 2002; Reimann et al., 2008). The use of these statistical methods allows the investigation of structures, trends, and associations of the elements studied, helping to understand the geological, physical, and anthropogenic processes that control the sediment geochemistry (Carranza, 2009; 2011; Filzmoser et al., 2009; Filzmoser et al., 2012; Grunsky, 2010; Lapworth et al., 2012; Reimann et al., 2002; Reimann et al., 2008).

### 3.2.1 Exploratory data analysis

The application of summary statistics, boxplots and normality test constitutes the initial phase of exploratory data analysis, intended to identify predominant trends and structures within data sets (Grunsky, 2010). Fifty elements from stream sediment samples in study area were utilized for univariate statistics in this step. However, Au, B, Ge, In, Na, Re, S, Se, Ta, Te, and Ti were excluded for further multivariate statistical analyses and baseline establishment due to their failure to meet the requisite for detection levels of <30% of censored data (Marques et al., 2023). For parameters undergoing further analysis, we regard the ND value as half of the quantification limit of the analytical method (Sanford et al., 1993).

The Shapiro-Wilk test was conducted at a significance level of 0.05 to evaluate the normality of both raw and log-transformed datasets. In every instance, the results were below significance, confirming that geochemical data have a non-normal distribution due to multiple populations (Grunsky, 2010; Lapworth et al., 2012; Reimann et al., 2008).

Spearman's correlation (Spearman, 1904) estimates the link between two variables, yielding values between −1 and 1 that indicate the degree of association between them. Utilizing bivariate statistics enables the construction of a correlation matrix to elucidate the probable geochemical associations and provide insights into the elemental groups constituting the principal contributors in the multivariate phase (Reimann et al., 2008). Utilizing Spearman's correlation (Spearman, 1904), we can identify clusters of geochemical affinities by assessing the degree of link among each element and all others. Moreover, the methodology is crucial for utilizing multivariate statistics, hence improving the elucidation of system variance. Specific properties associated with geological processes can be delineated by identifying the principal correlations among the sampled components.

### 3.2.2 Factor analysis

Factor analysis is a multivariate statistical technique for interpreting complex geochemical datasets by reducing the dimensionality, transforming many correlated elemental concentration variables into a smaller set (Carranza, 2011; Marques et al., 2023; Reimann et al., 2002; Reimann et al., 2008; Saadati et al., 2020). This simplifies the multivariate data and reveals underlying geochemical processes or associations that are often not apparent from univariate analysis. In stream sediment analysis, these factors can represent distinct geological influences such as the presence of specific mineral types, weathering processes, or anthropogenic contamination, allowing for a more robust interpretation of the data's spatial patterns.

Factor analysis (FA) were applied as a multivariate method to reduce dimensionality and achieve a better interpretation of the main geochemical associations in stream sediments. The compositional data of stream sediments must be first transformed to avoid the closure effect and the incidence of spurious correlations, as the factor analysis relies on the covariance matrix (Grunsky and de Caritat, 2017; Grunsky and Caritat, 2020). For this purpose, the Center log-ratio (CLR) transformation is applied to achieve a multivariate normal distribution, thereby preventing the non-normality of geochemical data from impacting the covariance matrix (Aitchison, 1982; Aitchison et al., 2000; Reimann et al., 2008). The CLR transformation was applied using the equation that represents the logarithmic ratios for each component based on the geometric mean of all components. Then factor analysis was conducted using the principal component extraction approach and the varimax orthogonal rotation method to enhance result interpretation by simplifying the modified data matrix (Kaiser, 1958). The application required the utilization of the statistical method based on the Kaiser criterion (1958), which considers eigenvalues over 1 as significant.

### 3.2.3 Baseline values

The geochemical baseline methods are employed to evaluate the baseline values (BV) for 20 elements in the study region, including Al, Ca, Fe, K, Mg, Mn, P, As, Ba, Cd, Co, Cr, Cu, Light Rare Earth Elements (LREE), Ni, Pb, Th, U, V, and Zn (Table 1). The baseline

**TABLE 1** Descriptive statistics.

| Element | Unit | NDL | % <NDL | Mean | SD | MAD | CV |
|---|---|---|---|---|---|---|---|
| Al | % | <0.01 | 0 | 1.93 | 1.43 | 0.97 | 74.4 |
| As | mg kg$^{-1}$ | <1 | 3.1 | 6.13 | 4.90 | 3.35 | 80 |
| Au* | mg kg$^{-1}$ | <0.1 | 99 | - | - | - | - |
| B* | mg kg$^{-1}$ | <10 | 95.8 | - | - | - | - |
| Ba | mg kg$^{-1}$ | <50 | 0.2 | 103 | 106 | 52.4 | 103 |
| Be | mg kg$^{-1}$ | <0.1 | 0.9 | 1.11 | 1.23 | 0.60 | 111 |
| Bi | mg kg$^{-1}$ | <0.02 | 0 | 0.23 | 0.15 | 0.1 | 64.1 |
| Ca | % | <0.01 | 3.1 | 0.08 | 0.12 | 0.05 | 160 |
| Cd | mg kg$^{-1}$ | <0.01 | 8.3 | 0.15 | 1.59 | 0.17 | 1,090 |
| Ce | mg kg$^{-1}$ | <0.05 | 0 | 73.6 | 65.8 | 35.2 | 89.5 |
| Co | mg kg$^{-1}$ | <0.1 | 0 | 14.6 | 153 | 9.12 | 103 |
| Cr | mg kg$^{-1}$ | <1 | 0 | 55.3 | 164 | 40.1 | 297 |
| Cs | mg kg$^{-1}$ | <0.05 | 0 | 1.46 | 1.30 | 0.86 | 88.9 |
| Cu | mg kg$^{-1}$ | <0.50 | 0 | 24.6 | 14.5 | 9.69 | 58.9 |
| Fe | % | <0.01 | 0.6 | 3.9 | 2.14 | 1.58 | 54.8 |
| Ga | mg kg$^{-1}$ | <0.1 | 0 | 7.75 | 4.75 | 3.36 | 61.2 |
| Ge* | mg kg$^{-1}$ | <0.1 | 79.4 | - | - | - | - |
| Hf | mg kg$^{-1}$ | <0.05 | 20.4 | 0.19 | 0.22 | 0.14 | 119 |
| Hg | mg kg$^{-1}$ | <0.01 | 23.9 | 0.03 | 0.03 | 0.02 | 96.5 |
| In* | mg kg$^{-1}$ | <0.02 | 36.1 | - | - | - | - |
| K | % | <0.01 | 0.3 | 0.16 | 0.09 | 0.07 | 56.2 |
| La | mg kg$^{-1}$ | <0.1 | 0 | 32.1 | 28.4 | 16.2 | 88.3 |
| Li | mg kg$^{-1}$ | <1 | 6.9 | 6.42 | 55 | 3.71 | 78.8 |
| ∑LREE | mg kg$^{-1}$ | <0.01 | 0 | 106 | 92.8 | 50.9 | 87.8 |
| Mg | % | <0.01 | 3.3 | 0.1 | 0.15 | 0.07 | 159 |
| Mn | mg kg$^{-1}$ | <5 | 0 | 566 | 592 | 413 | 105 |
| Mo | mg kg$^{-1}$ | <0.05 | 0 | 0.94 | 1.31 | 0.59 | 139 |
| Na* | % | <0.01 | 92.7 | - | - | - | - |
| Nb | mg kg$^{-1}$ | <0.05 | 0.4 | 0.86 | 1.57 | 0.77 | 181 |
| Ni | mg kg$^{-1}$ | <0.50 | 0 | 23.8 | 62.3 | 15.9 | 262 |
| P | mg kg$^{-1}$ | <50 | 0.7 | 439 | 558 | 246 | 127 |
| Pb | mg kg$^{-1}$ | <0.20 | 0 | 20.2 | 21.6 | 9.14 | 107 |
| Rb | mg kg$^{-1}$ | <0.20 | 0 | 14.8 | 12.2 | 7.40 | 82.4 |
| Re* | mg kg$^{-1}$ | <0.1 | 100 | - | - | - | - |
| S* | % | <0.01 | 65.3 | - | - | - | - |
| Sb | mg kg$^{-1}$ | <0.05 | 0 | 0.57 | 1.75 | 0.36 | 309 |
| Sc | mg kg$^{-1}$ | <0.1 | 0 | 6.11 | 5.10 | 3.30 | 83.4 |
| Se* | mg kg$^{-1}$ | <1 | 93.3 | - | - | - | - |

(Continued on following page)

**TABLE 1** (*Continued*) Descriptive statistics.

| Element | Unit | NDL | % <NDL | Mean | SD | MAD | CV |
|---|---|---|---|---|---|---|---|
| Sn | mg $kg^{-1}$ | <0.30 | 0.3 | 1.59 | 1.56 | 0.78 | 98.2 |
| Sr | mg $kg^{-1}$ | <0.50 | 0.4 | 10.9 | 28.9 | 10 | 2,659 |
| Ta* | mg $kg^{-1}$ | <0.05 | 92.1 | - | - | - | - |
| Te* | mg $kg^{-1}$ | <0.05 | 67.5 | - | - | - | - |
| Th | mg $kg^{-1}$ | <0.1 | 0 | 9.11 | 11 | 51 | 121 |
| Ti* | % | <0.01 | 45.9 | - | - | - | - |
| U | mg $kg^{-1}$ | <0.05 | 0 | 1.21 | 1.21 | 0.62 | 100 |
| V | mg $kg^{-1}$ | <1 | 0 | 56 | 41.4 | 28 | 74.1 |
| W | mg $kg^{-1}$ | <0.1 | 28.4 | 0.32 | 0.64 | 0.27 | 201 |
| Y | mg $kg^{-1}$ | <0.05 | 0 | 8.56 | 5.81 | 4.04 | 67.8 |
| Zn | mg $kg^{-1}$ | <1 | 0 | 46.3 | 89 | 26.6 | 192 |
| Zr | mg $kg^{-1}$ | <0.5 | 0.9 | 9.27 | 10.7 | 6.35 | 116 |

*indicates parameters with %<NDL, above 30%.

was determined using the median ±2 × median absolute deviation (mMad), Tukey's Inner Fence (TIF), and percentile-based (90th percentile). The baseline will be represented by concentration ranges encompassing both the upper and lower limits, as delineated by various authors (Gałuszka, 2007; Gałuszka et al., 2013; 2015; Licht, 2020; Matschullat et al., 2000; Reimann et al., 2002; Reimann and de Caritat, 2005; Reimann and de Caritat, 2017; Salomão et al., 2019; Salomão, 2020).

Given the lack of a single, universally accepted method in literature, the approach using multiple statistical techniques was adopted to ensure the robustness of our results. This strategy allowed us to evaluate the consistency of the baseline concentrations derived from different statistical assumptions. This robust, multi-methodological approach reduces the uncertainty inherent in any single technique and provides a solid foundation for distinguishing between natural elemental variations and potential anthropogenic anomalies.

Given the lithological nature of stream sediments, the baseline was computed for each of the six main lithological units in the study area. The calculations were conducted using sampling points spatially arranged over the following lithologies: (a) Monte Carmelo Complex (CMC), (b) Abadia dos Dourados Complex and Araxá Group (CAA), (c) Canastra Group (CAN), (d) Ibiá Group (IBI), (e) Vazante Group (VAZ), and (f) Serra da Saudade Formation.

The mMAD is a more robust methodology that mitigates the influence of outliers by employing the median as a measure of central tendency. Also being a suitable methodology to substitute the ±2σ mean technique, considered as in disuse (Reimann and De Caritat, 2005; Salomão, 2020). We perform the calculation of mMAD using the logarithmic transformation, then retransform the data to the original scale after the analysis and define the geochemical baseline values using Equation 1.

$$\begin{aligned} MAD(y) &= 1.4826 \cdot mediani\left|yi - medianj\left(yj\right)\right| \therefore mMAD \\ &= 10\left(median(y) \pm 2 \cdot \left[MADy\right]\right) \end{aligned} \tag{1}$$

As an initial requirement, the TIF method also requires that the data be previously transformed into the logarithmic scale (log10), prior to calculating the lower (LL) and upper (UL) baseline limits using Equations 2 and 3. Upon calculation, the final value is converted back to the original data scale, whether in mg.$kg^{-1}$ or % and, thereby establishing the baseline value.

$$TIFLL = 10\left(Q1 - 1,5 \cdot AIQ\right) \tag{2}$$

$$TIFUL = 10\left(Q3 + 1,5 \cdot AIQ\right) \tag{3}$$

Where: Q1 = 25th Quartile; Q2 = 75th Quartile; AIQ = Q2 – Q1.

# 4 Results

## 4.1 Exploratory data analysis and spatial distribution

The research area comprises six primary lithological units whose characteristics influence elemental behavior in the geochemical domain, as shown in the descriptive statistics (Table 1), boxplots (Figure 3) and the spatial distribution maps (Figure 4). The stream sediments originating from crystalline rocks and higher metamorphic grades, such as the Monte Carmelo and Abadia dos Dourados Complexes and the Araxá Group, exhibit higher median values for major elements such as K and Mg within study area (Pinho et al., 2017). Metasedimentary units like the Canastra, Ibiá, Vazante, and Bambuí groups demonstrate higher median values for Al, Fe, Ca, P, and Mn within the study area.

Elevated concentrations of Al are observed in the northwest and central-southern regions, where lateritic rock strata are substantial. Most rocks in the study area have high concentrations of Fe, except for the Monte Carmelo Complex. The spatial distribution of Fe reveals higher values in the Serra da Saudade formation, the Abadia Araxá Complex, the Serra de Santa Helena formation, and the Alkaline Complex of Santa Helena.

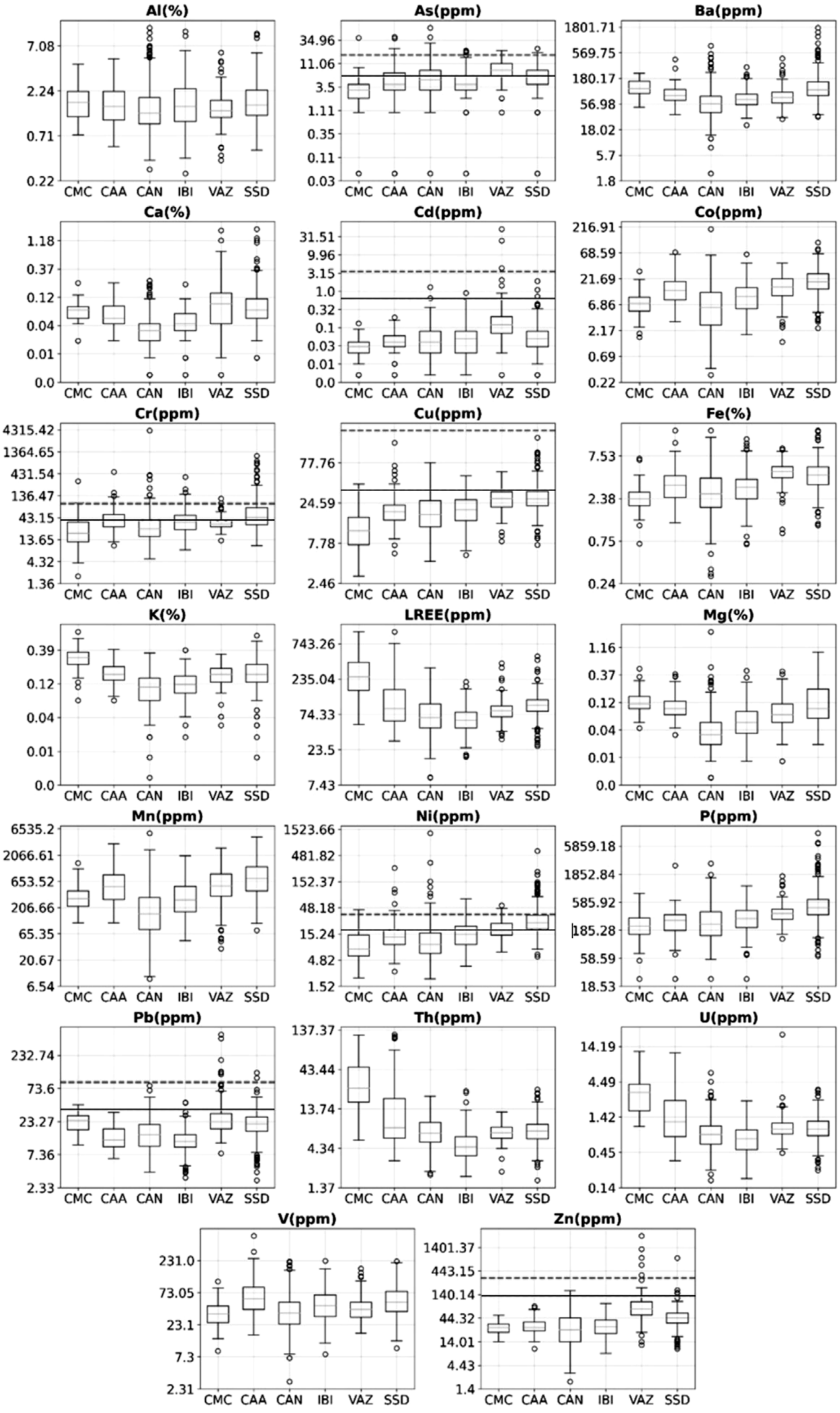

FIGURE 3
Boxplot graphs of the 6 main lithological units. Dashed and continuous lines represent respectively the upper and lower reference values of CONAMA 454/2012 resolution (Brasil, 2012).

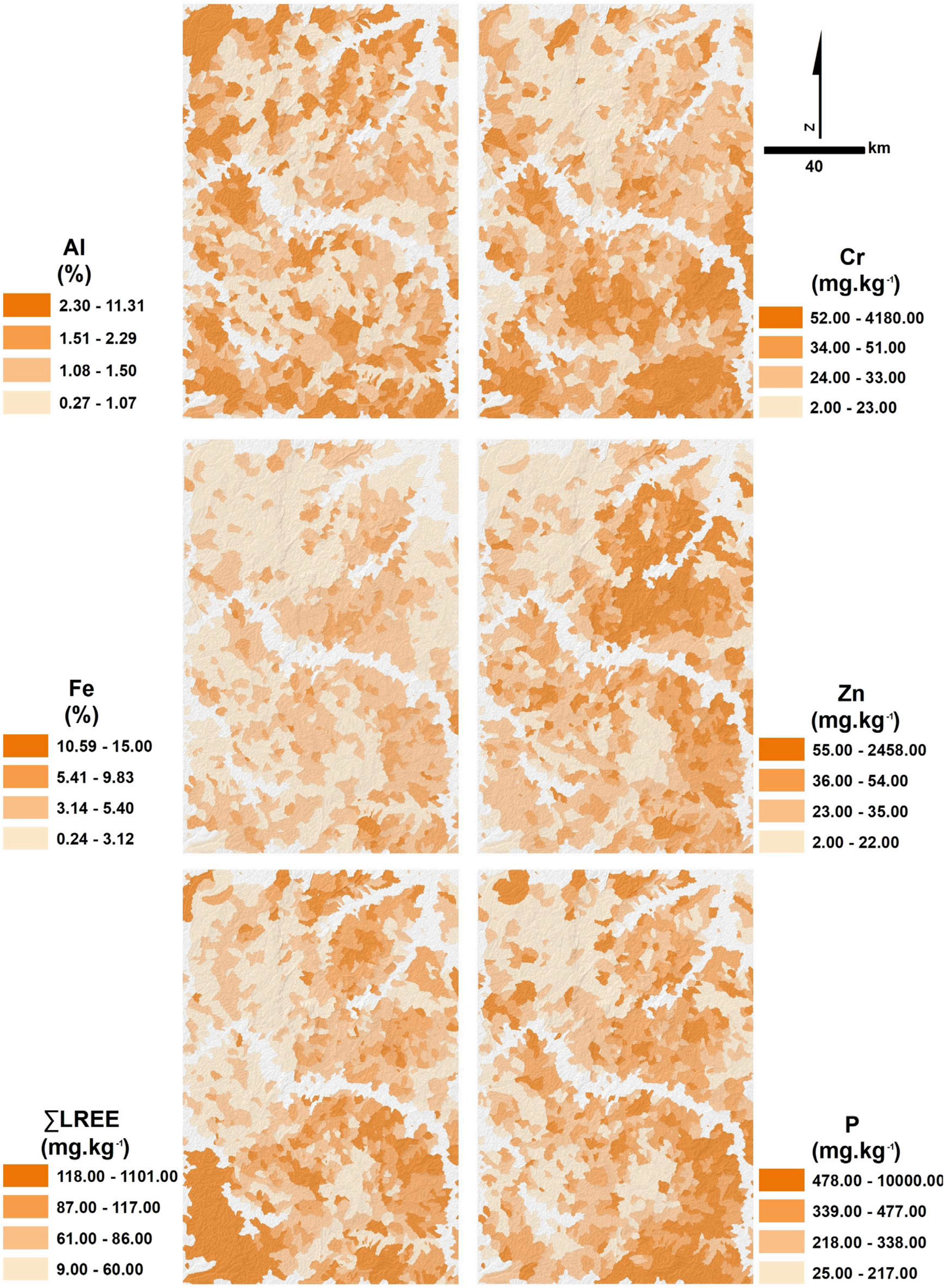

FIGURE 4
Spatial distribution of Al, Cr, Fe, Zn, LREE and P over the study area.

The Monte Carmelo and Abadia dos Dourados Complexes, along with the Araxá Group, have the highest median values for K. The Vazante and Bambuí Groups have elevated median values for Ca. The Serra de Santa Helena and Serra da Saudade formations exhibit elevated median values for P. Also, the Mata da Corda Group and the alkaline rocks of Serra Negra also exhibit high levels of P. Lastly, the highest median Mn values are found in the Vazante and Paranoá Groups and the Serra da

TABLE 2 Eingenvalues and variance of 6 main factors.

| Factors | Geochemistry association | Eigen values | Variance (%) |
|---|---|---|---|
| 1 | Al. Cs. Ga. Sn and V (−)/Co. Mg. Ni and Zn (+) | 6.06 | 26.4 |
| 2 | Cr and Ni (+)/K and Rb (−) | 4.30 | 18.7 |
| 3 | As e Fe (−) | 2.79 | 12.1 |
| 4 | Cd. Pb e Zn (+) | 1.59 | 6.91 |
| 5 | LREE. Th e U (+) | 1.37 | 5.95 |
| 6 | Ba. P e Sr (+) | 1.17 | 5.07 |

TABLE 3 Loadings of the main factors for stream sediment samples.

| Element | Factor 1 | Factor 2 | Factor 3 | Factor 4 | Factor 5 | Factor 6 |
|---|---|---|---|---|---|---|
| Al (CLR) | −0.91* | 0.06 | −0.04 | −0.02 | −0.11 | −0.08 |
| As (CLR) | 0.07 | −0.14 | −0.82* | 0.20 | −0.11 | −0.02 |
| Ba (CLR) | 0.46 | −0.17 | 0.21 | −0.44 | −0.02 | 0.42 |
| Ca (CLR) | 0.27 | −0.18 | 0.31 | 0.10 | −0.25 | 0.57* |
| Cd (CLR) | 0.13 | 0.17 | 0.12 | 0.71* | −0.27 | 0.06 |
| Co (CLR) | 0.81 | 0.09 | −0.10 | −0.16 | −0.24 | −0.06 |
| Cr (CLR) | −0.18 | 0.77* | 0.15 | −0.36 | −0.22 | −0.15 |
| Cs (CLR) | −0.57 | −0.44 | 0.29 | −0.14 | 0.21 | −0.24 |
| Fe (CLR) | 0.23 | 0.18 | −0.73* | −0.18 | −0.27 | −0.09 |
| Ga (CLR) | −0.83* | 0.14 | 0.01 | −0.07 | 0.10 | −0.22 |
| K (CLR) | 0.31 | −0.85* | 0.01 | −0.03 | −0.04 | −0.11 |
| LREE (CLR) | −0.01 | −0.12 | 0.18 | 0 | 0.86* | 0.02 |
| Mg (CLR) | 0.60* | −0.22 | 0.49 | −0.14 | −0.26 | 0.10 |
| Ni (CLR) | 0.52* | 0.60* | 0.09 | −0.23 | −0.31 | 0.02 |
| P (CLR) | −0.05 | 0.34 | −0.29 | 0.01 | −0.20 | 0.72* |
| Pb (CLR) | −0.02 | −0.21 | −0.12 | 0.77* | 0.13 | −0.16 |
| Rb (CLR) | −0.03 | −0.87* | 0.19 | −0.19 | 0.20 | −0.14 |
| Sn (CLR) | −0.74* | 0.12 | 0.27 | −0.15 | 0.22 | −0.09 |
| Sr (CLR) | 0.30 | 0.09 | 0.24 | −0.40 | 0.07 | 0.65* |
| Th (CLR) | −0.10 | −0.25 | −0.04 | −0.13 | 0.81* | −0.26 |
| U (CLR) | −0.32 | −0.11 | 0.16 | −0.04 | 0.79* | −0.08 |
| V (CLR) | −0.61* | 0.49* | 0.01 | −0.27 | −0.26 | −0.15 |
| Zn (CLR) | 0.54* | −0.14 | −0.13 | 0.46* | −0.33 | 0.07 |

Values with * displays the best correlations of the variables with the factor.

Saudade Formation. Quaternary units also show anomalous P concentrations.

Anomalous concentrations of Ni and Cr are located over ultramafic intrusive alkaline rocks, specifically at the Serra Negra and Chapada dos Pilões Formations. Other anomalies are also observed above the Serra da Saudade Formation, from the Bambuí and Mata da Corda Groups. The spatial distribution of Zn resembles that of Cr. The dolomitic rocks of the Serra do Garrote Formation (Vazante Group) show the highest concentrations of Zn.

The sub-basins comprising the lithology of the Serra de Santa Helena Formation, including the Rocinha and Lagamar deposits in the center region of the research area, exhibit anomalies in phosphorus levels. Although increased levels of phosphorus are found over specific lithologies, an anomaly is observed in the northwestern section of the study area over Cenozoic deposits.

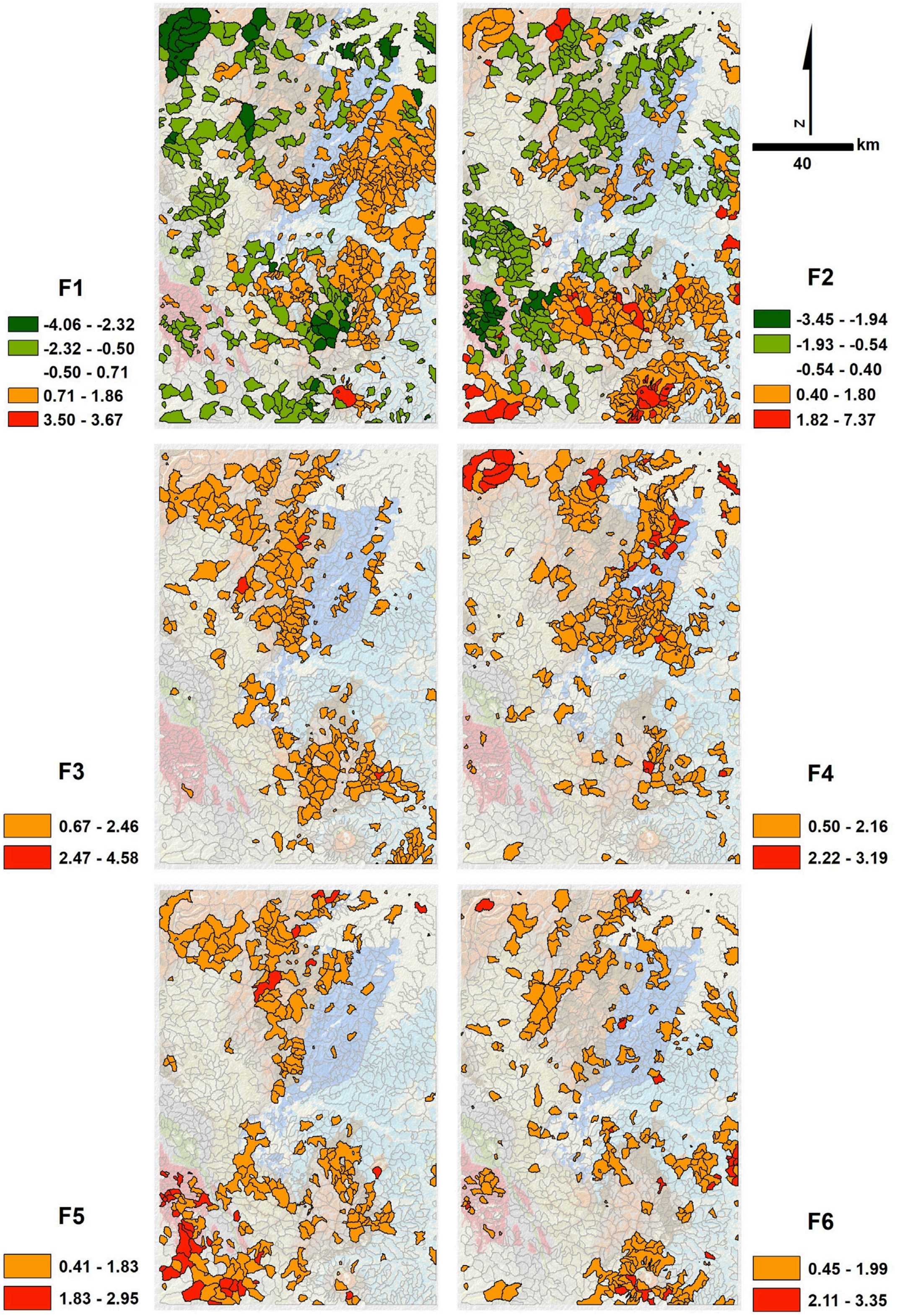

FIGURE 5
Spatial distribution of the 6 main factors by sub-basins over the geological basemap from Figure 2.

The Monte Carmelo and Abadia dos Dourados Complexes along with the Araxá Group, have the highest median values for elements with large ionic radii, such as Ba, Cs, and Rb. The Monte Carmelo Complex, the Paranoá Group's metasedimentary units, and the Serra da Saudade Formation exhibit the highest median values for Sr.

Among the elements with high ionic valences, including Nb, Th, U, the Light Rare Earth Elements (LREE; La-Ce) and Y exhibit their highest median ranges for the Monte Carmelo and Abadia dos Dourados Complexes, as well as the Araxá Group. The elements Hf and Zr, exhibit their highest median ranges within the metasedimentary units, specifically for Hf in the Serra da Saudade Formation and Zr in the Paranoá Group.

## 4.2 Multivariate geochemical patterns

Factor analysis reveals six components that explain 75.1% of the variance in the compositional system of stream sediments (Table 2). Factor 1 accounts for 26.4% of the total variance and exhibits strong positive loadings for Co, Mg, Ni, and Zn (Table 3). Conversely, negative loadings show an association among Al, Cs, Ga, Sn, and V. The positive loadings of Factor 1 are spatially distributed (Figure 5) within the Vazante, the Bambuí, and the Mata da Corda Groups, with the highest values in the Serra Negra Intrusive Suite region. The northwest region shows negative loadings of Factor 1, associated with Cenozoic and laterite coverings, while at the northeast portion occurs over detrital sedimentary deposits.

Factor 2 accounts for 18.7% of the overall system variance. It exhibits a strong positive association for Cr, Ni, and V, while the negative values represent the relationship between Cs, K, and Rb. The positive loadings of Factor 2 indicate the spatial arrangement of elements from Serra Negra Intrusive Suite rocks, and the Mata da Corda group. Positive values are also observed over rocks of the Ibiá and Canastra Groups and Cenozoic laterite covers. The negative counterpart of the factor 2 values comprises the association of Cs, K and Rb elements within the following lithological units: Monte Carmelo and Abadia dos Dourados complexes; the mica schists of the Araxá Group; the Serra do Poço Verde and Serra da Lapa Formations of the Vazante group; the Chapada dos Pilões and Paracatu Formations of the Canastra Group and the Serra da Saudade Formation of the Bambuí Group.

Factor 3 represents 12.1% of the system's total variance and indicates the correlation between As and Fe over rocks from Morro do Ouro member (Paracatu Formation). While Factor 4, accounts for 6.91% of the system's total variance, has positive loadings that correspond to the association between Cd, Pb, and Zn. The Light Rare Earth Elements (LREE), Th, and U have significant positive associations, as indicated by factor 5, which accounts for 5.95% of the total variance in the system. Another group with significant values for this association is spatially distributed over rocks of the Ibiá Group. Factor 6, representing 5.07% of the total variance of the system, indicates relationships for Ba, P and Sr. Positive loadings are observed near rocks of the Serra Negra Intrusive Suite, over the Mata da Corda Group, and in the northwest portion of the study area.

## 4.3 The influence of lithology on geochemical baseline values

The baseline values calculated by the main lithological units allow for the evaluation of geological control on the element naturally distributed in the stream sediments. The values suggested for the baseline (Table 4) provided more conservative estimates for the mMad approach compared to the TIF method. Certain values exceed the preventive and investigation values established by CONAMA resolution No. 454/2012 (Brasil, 2012).

The group of major elements exhibited baseline values exceeding the crustal average in all examined lithologies for Iron and Manganese (Rudnick and Gao, 2003). The Phosphorus values exceed the reference levels for the Canastra Group and Serra da Saudade Formation. The baseline values for trace elements, some of which are potentially toxic ones, exceed the legal Quality Reference Values (Brasil, 2012) in all lithological units for As, Ba, Co, Cr and Ni. As for Cu, higher values occur for the Araxá Abadia Complex, Canastra Group, Ibiá Group, Vazante Group and Serra da Saudade Formation. The element Co exceeds the Investigation Value for the rocks of Canastra Group.

# 5 Discussion

The exploratory data analysis confirms a strong relationship between elemental concentrations and the underlying lithology. The elevated concentrations of K and Mg in sediments from crystalline and high-grade metamorphic rocks, such as the Monte Carmelo and Abadia dos Dourados Complexes, are likely influenced by granitoid and alkaline rocks (Pereira and Fuck, 2005; Uhlein et al., 2012). The high levels of Ca in the Vazante and Bambuí Groups are consistent with the presence of carbonate rocks (Dias et al., 2018; Moreira, 2015). Similarly, the elevated P in the Serra de Santa Helena Formation is linked to known phosphate deposits, such as Lagamar region (Moreira, 2015) and the alkaline intrusions of Serra Negra, due to the presence of apatite in the rocks' mineralogy. Conversely, quaternary units exhibit anomalous P concentrations, a phenomenon associated with agricultural activities, particularly soybean planting (Rawlins, 2011; Steegen et al., 2001; Yang et al., 2010). While the high Mn values in the Vazante and Paranoá Groups and the Serra da Saudade Formation may be due to hydrothermal processes (Cevik et al., 2021).

The spatial distribution of Al, Fe, Cr, and V anomalies is related to lateritic cover, suggesting a strong influence of pedogenetic processes where these elements are adsorbed or co-precipitated in clay minerals and oxyhydroxides (Yariv and Cross, 1979; Yariv and Cross, 2001). Ni and Cr linked to ultramafic intrusive alkaline rocks of the Serra Negra and Chapada dos Pilões Formations and also Bambuí and Mata da Corda Group, indicating influence from alkaline metatuffs mineralogy, such as olivine and pyroxene (Klein and Dutrow, 2007; Asniar et al., 2019). The dolomitic rocks of the Serra do Garrote Formation, part of the Vazante group, contain the highest concentrations of Zn, where the main silicate zinc mines are located (Fernandes et al., 2021).

Ba, Cs, and Rb may be associated with the chemistry of primary minerals, such as feldspars (Klein and Dutrow, 2007) from Monte Carmelo and Abadia dos Dourados Complexes along with the Araxá Group. Hydrothermal processes are most likely the cause of the unusual levels of these elements found in the metasedimentary units, primarily in the Vazante Group and Serra da Saudade Formation (Cevik et al., 2021). Also, the Sr is presented in locations influenced by hydrothermalism, as well as in primary minerals from Monte Carmelo Complex and carbonate rocks (Cevik et al., 2021). The concentrations of LREE, U, and Th are elevated relative to the UCC,

**TABLE 4** Baseline values by lithological units according to percentile.

| Elm. | Unit | CMC | | | CAA | | | CAN | | |
|---|---|---|---|---|---|---|---|---|---|---|
| | | Q90th | TIF | mMAD | Q90th | TIF | mMAD | Q90th | TIF | mMAD |
| Al | % | 3.17 | 6.22 | 4.42 | 3.02 | 7.02 | 4.56 | 3.73 | 5.32 | 3.47 |
| Ca | % | 0.11 | 0.19 | 0.19 | 0.13 | 0.28 | 0.14 | 0.08 | 0.11 | 0.1 |
| Fe | % | 3.75 | 4.96 | 3.99 | 6.69 | 10.82 | 8.35 | 5.79 | 13.7 | 8.61 |
| K | % | 0.52 | 0.68 | 0.58 | 0.28 | 0.43 | 0.36 | 0.19 | 0.47 | 0.28 |
| Mg | % | 0.24 | 0.35 | 0.28 | 0.22 | 0.31 | 0.21 | 0.07 | 0.2 | 0.14 |
| Mn | mg.kg$^{-1}$ | 560 | 1,215 | 824 | 1,318 | 4,712 | 2,662 | 592 | 2,741 | 1,303 |
| P | mg.kg$^{-1}$ | 372 | 900 | 613 | 442 | 953 | 759 | 576 | 1720 | 991 |
| As | mg.kg$^{-1}$ | 6.19* | 14.9* | 9.96* | 10.1* | 24.9** | 21** | 14* | 34.8** | 22.7** |
| Ba | mg.kg$^{-1}$ | 197 | 385 | 263 | 129 | 226 | 171 | 123 | 242 | 162 |
| Cd | mg.kg$^{-1}$ | 0.06 | 0.11 | 0.10 | 0.09 | 0.17 | 0.09 | 0.14 | 0.64* | 0.31 |
| Co | mg.kg$^{-1}$ | 15 | 24.2 | 16.4 | 36.4 | 67.6 | 44.1 | 21.1 | 106 | 49.4 |
| Cr | mg.kg$^{-1}$ | 53.2* | 192** | 95.8** | 89.2* | 132** | 94** | 64.7* | 139** | 79.7* |
| Cu | mg.kg$^{-1}$ | 20.8 | 54.1* | 36.9* | 35.3 | 44.7* | 37.2* | 36.8* | 81.2* | 53.3* |
| LREE | mg.kg$^{-1}$ | 518 | 1776 | 1,004 | 297 | 807 | 350 | 140 | 339 | 209 |
| Ni | mg.kg$^{-1}$ | 24.3* | 60.6** | 41.3** | 28* | 49.6** | 35.2** | 27.7* | 62.6** | 39.2** |
| Pb | mg.kg$^{-1}$ | 32.2 | 61.1* | 44.4* | 22.4 | 46.3* | 29.7 | 29.8 | 65.7* | 45.5* |
| Th | mg.kg$^{-1}$ | 66.9 | 226 | 104 | 34.6 | 108 | 30.5 | 12.1 | 22.2 | 15.9 |
| U | mg.kg$^{-1}$ | 6.19 | 16.3 | 10.6 | 3.97 | 14.9 | 7.6 | 1.54 | 2.55 | 1.92 |
| V | mg.kg$^{-1}$ | 65 | 112 | 83.2 | 139 | 287 | 190 | 89.7 | 174 | 113 |
| Zn | mg.kg$^{-1}$ | 38.4 | 60.6 | 45.5 | 53 | 70.8 | 55.7 | 64.7 | 256* | 139* |
| Elm. | Unit | IBI | | | VAZ | | | SSD | | |
| | | Q90th | TIF | mMAD | Q90th | TIF | mMAD | Q90th | TIF | mMAD |
| Al | % | 3.42 | 8.58 | 5.35 | 2.51 | 3.44 | 2.53 | 3.29 | 6.14 | 3.95 |
| Ca | % | 0.07 | 0.17 | 0.11 | 0.24 | 0.92 | 0.51 | 0.18 | 0.36 | 0.20 |
| Fe | % | 5.23 | 8.84 | 7.5 | 6.54 | 8.81 | 7.57 | 7.26 | 11.59 | 8.94 |
| K | % | 0.2 | 0.38 | 0.28 | 0.25 | 0.43 | 0.36 | 0.29 | 0.6 | 0.38 |
| Mg | mg.kg$^{-1}$ | 0.13 | 0.35 | 0.2 | 0.14 | 0.36 | 0.2 | 0.31 | 1.33 | 0.51 |
| Mn | mg.kg$^{-1}$ | 932 | 2,880 | 1,628 | 1,393 | 3,902 | 2,305 | 1889 | 6,336 | 3,646 |
| P | mg.kg$^{-1}$ | 519 | 1,217 | 821 | 562 | 820 | 654 | 1,229 | 1716 | 1,220 |
| As | mg.kg$^{-1}$ | 9.49* | 17* | 9.37* | 15* | 30.4** | 20.5** | 10* | 22.6** | 19.9** |
| Ba | mg.kg$^{-1}$ | 107 | 178 | 140 | 127 | 202 | 157 | 244 | 388 | 263 |
| Cd | mg.kg$^{-1}$ | 0.11 | 0.64* | 0.23 | 0.47 | 1.03* | 0.59 | 0.13 | 0.35 | 0.2 |
| Co | mg.kg$^{-1}$ | 22.6 | 59.5 | 40.1 | 29.2 | 68.9 | 44.5 | 36.4 | 75.7 | 52.2 |
| Cr | mg.kg$^{-1}$ | 72.5* | 154** | 106** | 48* | 59.4* | 52.2* | 113** | 277** | 144** |
| Cu | mg.kg$^{-1}$ | 32 | 65* | 48.5* | 42.9* | 66.7* | 53.2* | 44.7* | 63.9* | 51.3* |
| LREE | mg.kg$^{-1}$ | 116 | 175 | 131 | 130 | 167 | 141 | 141 | 213 | 175 |
| Ni | mg.kg$^{-1}$ | 26.4* | 71.9** | 47.7** | 32* | 53.3** | 41.2** | 56.1** | 85.6** | 61.2** |

(Continued on following page)

TABLE 4 (*Continued*) Baseline values by lithological units according to percentile.

| Elm. | Unit | IBI | | | VAZ | | | SSD | | |
|---|---|---|---|---|---|---|---|---|---|---|
| | | Q90th | TIF | mMAD | Q90th | TIF | mMAD | Q90th | TIF | mMAD |
| Pb | mg.kg$^{-1}$ | 18.9 | 28.4 | 21.6 | 53.2* | 70.1* | 52* | 33.7 | 58.2* | 44.4* |
| Th | mg.kg$^{-1}$ | 8.65 | 14 | 10.6 | 9.66 | 13.6 | 11.4 | 10.7 | 16.9 | 13.9 |
| U | mg.kg$^{-1}$ | 1.36 | 2.51 | 1.75 | 1.44 | 2.03 | 1.71 | 1.58 | 2.48 | 1.92 |
| V | mg.kg$^{-1}$ | 96.5 | 213 | 147.1 | 70.8 | 119 | 87 | 109 | 224 | 154 |
| Zn | mg.kg$^{-1}$ | 52 | 105 | 75.2 | 167* | 254* | 169* | 72 | 118 | 94.7 |

TIF., and mMad methods. Elm, Element; CMC, monte carmelo complex; CAA, Araxá Group and Abadia Complex; CAN, canasta group; IBI, Ibiá Group; VAZ, vazante group; SSD, Serra da Saudade Formation. * (level 2) and ** (level) for values above Conama Resolution n°454/2012 thresholds.

whereas Y approximates the crustal average, supporting the hypothesis that these elements originate from resistant minerals (Klein and Dutrow, 2007).

Factor analysis effectively grouped elements based on their geochemical behavior. Factor 1 represents two distinct geochemical processes: positive loadings (Co, Mg, Ni, Zn) linked to the influence of hydrothermal zones along shear zone contacts and ultramafic rocks (Cevik et al., 2021), and negative loadings (Al, Cs, Ga, Sn, V) associated with Cenozoic and laterite deposits. The pedogenetic process of laterization, involving the adsorption or co-precipitation of clay minerals and aluminum oxyhydroxides, could potentially influence these factors (Yariv and Cross, 1979; Yariv and Cross, 2001). The spatial distribution of positive loadings of Factor 2 (Cr, Ni and V) over Serra Negra Intrusive Suite rocks and Mata da Corda may be linked with the mafic and ultramafic rocks, as well as the occurrence of resistant minerals like magnetite (Klein and Dutrow, 2007). Positive loadings were also observed over rocks of the Ibiá and Canastra Groups and may be influenced by the presence of kimberlites. The negative association of Factor 2 (Cs, K, Rb) highlights the influence of k-feldspars and micas in certain lithologies (Klein and Dutrow, 2007), reaffirming the role of hydrothermal processes over Monte Carmelo and Abadia dos Dourados complexes and the Araxá, Vazante, Canastra and Bambuí Groups.

The associations in the remaining factors provide further insights. Factor 3 (As, Fe) may be linked to sulfide minerals like arsenopyrite from a mineral paragenesis related to Au deposits (Vilor et al., 2014). The positive loadings of Factor 4 (Cd, Pb, Zn) are strongly influenced by the well-known silicate zinc mineralization in the Vazante Province. Factor 5 (LREE, Th, U) indicates the presence of heavy-resistant minerals like zircon and monazite inherited from the parental rocks (Klein and Dutrow, 2007). Finally, Factor 6 (Ba, P, Sr) reflects lithological sources such as apatite in alkaline intrusions and potentially anthropogenic influences of phosphorus from agricultural fertilizers, particularly in the laterite plateaus.

Establishing the lithology-based baseline calculation highlights the essential relationships between elements and distinct lithotypes, providing a more reliable foundation than a single, regional baseline. The method reveals that elevated concentrations of certain elements are naturally present, such as Co in the Canastra Group, and Cr and Ni in the Serra da Saudade Formation. The baseline values for sediments derived from crystalline and higher metamorphic grade rocks, including the Monte Carmelo Complex, Abadia dos Dourados and the Araxá Group exhibit elevated concentrations of elements such as Th, U and V and Light Rare Earth Elements (LREE). Conversely, metasedimentary rocks, including the Canastra, Vazante, Ibiá and Serra da Saudade formations exhibit elevated baseline values for the elements Mg, P, Cd, Cu and Zn. The largest range of P baseline is found in sediments from the Serra da Saudade formation and Canastra group, the former being a phosphate mineralization. The baselines values offer a significant regional database for monitoring potentially toxic elements (PTE) within the river basin and function as an effective instrument for river impact management.

## 6 Conclusion

This study successfully applied a multi-methodological approach, combining multivariate statistical analysis with a lithology-based baseline calculation, to characterize the geochemical signatures of stream sediments within the study's metallogenetic province. The primary objectives of reducing data dimensionality and establishing reliable geochemical baseline values were fully achieved. This approach effectively achieved the core objectives of simplifying a high-dimensional dataset and differentiating natural elemental enrichment from potential anthropogenic contamination. The Factor Analysis proved crucial for simplifying the complex dataset, reducing the 20 analyzed elements into six primary factors that collectively account for 75.12% of the total variance. These factors reveal distinct geochemical associations directly linked to specific geological and environmental processes. Factors highlighted the strong influence of mafic/ultramafic rocks (Co, Ni, Cr, Zn) associated with the Serra Negra Intrusive Suite, and hydrothermal activity along shear zones. Furthermore, associations of LREE, Th, and U confirmed the contribution of heavy-resistant minerals inherited from the parental rocks. The analysis confirmed the widespread impact of laterization (Al, Fe, V) and identified the geochemical signature of specific mineralization occurrences, such as the silicate zinc deposits (Zn, Cd, Pb) in the Vazante Group.

The spatial distribution of phosphorus (P), particularly observed in Factor 6, reveals a complex interplay between natural sources (phosphate mineralization and alkaline rocks) and localized anthropogenic dispersal associated with agricultural activity in the laterite plateaus. Crucially, the lithology-specific geochemical baseline demonstrates the strong control of the underlying geology on element concentrations. By calculating the baseline for each major lithological unit, the results showed that the elevated concentrations of elements like As, Co, Cr, and Ni which frequently exceed established national Quality Reference Values (CONAMA 454/2012), are fundamentally natural geological phenomena. In conclusion, this research provides a robust, data-driven framework for managing environmental resources in geologically enriched areas. The established lithology-based baselines serve as an indispensable reference database for monitoring potentially toxic elements (PTEs) and for accurately assessing environmental risk, thereby supporting effective land use planning and regulatory decision-making in the region.

## Data availability statement

Publicly available datasets were analyzed in this study. This data can be found here: https://rigeo.sgb.gov.br/handle/doc/19397.

## Author contributions

RA: Conceptualization, Data curation, Formal Analysis, Funding acquisition, Investigation, Methodology, Project administration, Resources, Software, Supervision, Validation, Visualization, Writing – original draft, Writing – review and editing. EM: Conceptualization, Data curation, Formal Analysis, Funding acquisition, Investigation, Methodology, Project administration, Resources, Software, Supervision, Validation, Visualization, Writing – review and editing. ÚR: Conceptualization, Supervision, Validation, Writing – review and editing. ES-F: Formal Analysis, Investigation, Methodology, Supervision, Validation, Writing – review and editing. GA: Formal Analysis, Investigation, Methodology, Writing – review and editing. IM: Formal Analysis, Investigation, Visualization, Writing – review and editing. GS: Conceptualization, Data curation, Formal Analysis, Investigation, Methodology, Software, Supervision, Validation, Visualization, Writing – review and editing, Funding acquisition.

## Funding

The authors declare that financial support was received for the research and/or publication of this article. Data acquisitions were financially supported by the Geological Survey of Brazil (SGB) through the Paracatu–Vazante Project from the Geology of Brazil Program (PGB). Funding for the research submission was kindly granted by Instituto Tecnológico Vale (ITV). Scholarships were financially supported by the Instituto Tecnológico Vale (ITV) and managed by the Fundação Amparo e Desenvolvimento da Pesquisa–FADESP ((#339020.02 to RA).

## Conflict of interest

The authors declare that the research was conducted in the absence of any commercial or financial relationships that could be construed as a potential conflict of interest.

## Generative AI statement

The authors declare that no Generative AI was used in the creation of this manuscript.

Any alternative text (alt text) provided alongside figures in this article has been generated by Frontiers with the support of artificial intelligence and reasonable efforts have been made to ensure accuracy, including review by the authors wherever possible. If you identify any issues, please contact us.

## Publisher's note

## References

Aitchison, J. (1982). The statistical analysis of compositional data. *J. R. Stat. Soc. Ser. B Methodol.* 44 (2), 139–160. doi:10.1111/j.2517-6161.1982.tb01195.x

Aitchison, J., Barceló-Vidal, C., Martín-Fernández, J. A., and Pawlowsky-Glahn, V. (2000). Logratio analysis and compositional distance. *Math. Geol.* 32 (3), 271–275. doi:10.1023/a:1007529726302

Albanese, S., De Vivo, B., Lima, A., and Cicchella, D. (2007). Geochemical background and baseline values of toxic elements in stream sediments of Campania region (italy). *J. Geochem. Explor.* 93 (1), 21–34. doi:10.1016/j.gexplo.2006.07.006

Almeida, F. F. M. (1981). O Cráton do Paramirim e suas relações com o do São Francisco. *An. do Simpósio sobre Cráton do São Francisco suas Faixas Marginais* 1, 1–10.

Almeida, G. S., Salomão, G., Dall'Agnol, R., Tarantino, R., Medeiros Filho, L., Sahoo, P., et al. (2024). Hydrogeochemical process, evaluation of pollution source apportionment and baseline characteristics of surface water in the quadrilátero ferrífero, Minas Gerais, Brazil. *Eval. Pollut. Source Apportionment Baseline Charact. Surf. Water Quadrilátero Ferrífero, Minas Gerais, Braz.*

APHA (2017). *Standard methods for the examination of water and wastewater*. 23rd ed. Washington DC: American Public Health Association.

Asniar, N., Purwana, Y. M., and Surjandari, N. S. (2019). "Tuff as rock and soil: review of the literature on tuff geotechnical, chemical and mineralogical properties around the world and in Indonesia. AIP Publishing LLC.

Babu, S. S., Prajith, A., Rao, V. P., Mohan, M. R., Ramana, R. V., and Sree, N. S. (2023). Composition of river sediments from Kerala, southwest India: inferences on lateritic weathering. *J. Earth Syst. Sci.* 132 (4), 150. doi:10.1007/s12040-023-02153-7

Boente, C., Albuquerque, M., Fernández-Braña, A., Gerassis, S., Sierra, C., and Gallego, J. (2018). Combining raw and compositional data to determine the spatial patterns of potentially toxic elements in soils. *Sci. Total Environ.* 631–632, 1117–1126. doi:10.1016/j.scitotenv.2018.03.048

Brasil (2009). *Resolução CONAMA n° 420, de 28 de dezembro de 2009*. Brasília: Diário Oficial da União.

Brasil (2012). *Resolução CONAMA n° 454, de 01 de novembro de 2012*. Brasília: Diário Oficial da União.

Buccianti, A., and Grunsky, E. (2014). Compositional data analysis in geochemistry: are we sure to see what really occurs during natural processes? *J. Geochem. Explor.* 141, 1–5. doi:10.1016/j.gexplo.2014.03.022

Buccianti, A., Egozcue, J. J., and Pawlowsky-Glahn, V. (2008). Another look at the chemical relationships in the dissolved phase of complex river systems. *Math. Geosci.* 40, 475–488. doi:10.1007/s11004-008-9168-2

Caby, R., Sial, A. N., Arthaud, M., and Vauchez, A. (1991). "Crustal evolution and the Brasiliano orogeny in northeast Brazil," in *The West African orogens and circum-atlantic correlatives*. Editors R. D. Dallmeyer and J. P. Lécorché (Berlin, Heidelberg: Springer), 373–397. doi:10.1007/978-3-642-84153-8_16

Caritat, P. de, Reimann, C., Smith, D. B., and Wang, X. (2018). Chemical elements in the environment: multi-element geochemical datasets from continental-to national-scale surveys on four continents. *Appl. Geochem.* 89, 150–159. doi:10.1016/j.apgeochem.2017.11.010

Carranza, E. J. M. (2009). "Exploratory analysis of geochemical anomalies," in *Geochemical anomaly and mineral prospectivity mapping in GIS*. Editor E. J. M. Carranza (Amsterdam: Elsevier), 119–166.

Carranza, E. J. M. (2011). Analysis and mapping of geochemical anomalies using logratio-transformed stream sediment data with censored values. *J. Geochem. Explor.* 110 (2), 167–185. doi:10.1016/j.gexplo.2011.05.007

Çavdar, B., Günay, K., and Mutlu, H. (2025). Stream sediment and soil geochemistry of the largest volcanogenic massive sulfide deposit in Türkiye, Karaburun deposit (Central Pontides). *J. Geochem. Explor.* 277, 107816. doi:10.1016/j.gexplo.2025.107816

CETESB (Companhia Ambiental do Estado de São Paulo) (2018). Qualidade das águas interiores no Estado de São Paulo. Apêndice D. Índices Qual. das Águas. *São Paulo CETESB*. Available online at: https://aguasinteriores.cetesb.sp.gov.br/wp-content/uploads/sites/32/2013/11/10.pdf (Accessed August 10, 2025).

Cevik, I. S., Olivo, G. R., and Ortiz, J. M. (2021). A combined multivariate approach analyzing geochemical data for knowledge discovery: the Vazante–Paracatu Zinc District, Minas Gerais, Brazil. *J. Geochem. Explor.* 221, 106696. doi:10.1016/j.gexplo.2020.106696

Cheng, Q. (2007). Mapping singularities with stream sediment geochemical data for prediction of undiscovered mineral deposits in Gejiu, Yunnan Province, China. *Ore Geol. Rev.* 32 (1-2), 314–324. doi:10.1016/j.oregeorev.2006.10.002

Comas, M., and Thió-Henestrosa, S. (2011). "CoDaPack 2.0: a stand-alone, multi-platform compositional software," in *Proceedings of the 4th international workshop on compositional data analysis*. Editors J. J. Egozcue, R. Tolosana-Delgado, and M. I. Ortego (Spain: Sant Feliu de Guíxols).

Dardenne, M. A. (2000). "The Brasília fold belt," in *Tectonic evolution of South America*. Editors U. G. Cordani, E. J. Milani, A. Thomaz Filho, and D. A. Campos (Rio de Janeiro: 31st International Geological Congress), 231–263.

Dardenne, M. A., Freitas-Silva, F. H., Nogueira, G. S. M., and Souza, J. C. F. (1997). "Depósitos de fosfato de Rocinha e Lagamar, Minas Gerais," Brasília: CPRM/DNPM, 113–122.

Darnley, A. G. (1995). *A global geochemical database for environmental and resource management: recommendations for international geochemical mapping*. UNESCO. Final Report of IGCP Project 259.

Darnley, A. G., and Garrett, R. G. (1990). International Geochemical Mapping-IGCP Project 259. *J. Geochem. Explor.* 39 (1-2), 1–253.

de Vicq, R., Matschullat, J., Leite, M. G. P., Nalini, H. A., Jr., and Mendonça, F. P. C. (2015). Iron Quadrangle stream sediments, Brazil: geochemical maps and reference values. *Environ. Earth Sci.* 74 (5), 4407–4417. doi:10.1007/s12665-015-4508-2

Dellamatrice, P. M., and Monteiro, R. T. R. (2014). Principais aspectos da poluição de rios brasileiros por pesticidas. *Rev. Bras. De. Eng. Agrícola E Ambient.* 18 (12), 1296–1301. doi:10.1590/1807-1929/agriambi.v18n12p1296-1301

Dias, P. H. A., Sotero, M. P., Matos, C. A., Marques, E. D., Marinho, M. de S., and Couto Junior, M. A. (2018). "Área de Relevante Interesse Mineral - ARIM: distrito mineral de Paracatu-Unaí (Zn-Pb-Cu)," CPRM - Serviço Geológico do Brasil. Available online at: https://rigeo.sgb.gov.br/handle/doc/19396.

Felix, F. F., Navickiene, S., and Dórea, H. S. (2007). Poluentes orgânicos persistentes (POPs) como indicadores da qualidade dos solos. *Rev. Fapese* 3 (2), 39–62.

Fernandes, N. A., Olivo, G. R., Layton-Matthews, D., Voinot, A., Chipley, D., Leybourne, M., et al. (2021). Metal sources in the Proterozoic Vazante-Paracatu sediment-hosted Zn District, Brazil: constraints from Pb isotope compositions of meta-siliciclastic units. *Can. Mineralogist* 59 (5), 1187–1205. doi:10.3749/canmin.2000055

Filzmoser, P., Hron, K., and Reimann, C. (2009). Principal component analysis for compositional data with outliers. *Environmetrics* 20 (6), 621–632. doi:10.1002/env.966

Filzmoser, P., Hron, K., and Reimann, C. (2012). Interpretation of multivariate outliers for compositional data. *Comput. and Geosciences* 39, 77–85. doi:10.1016/j.cageo.2011.06.014

Gałuszka, A. (2007). A review of geochemical background concepts and an example using data from Poland. *Environ. Geol.* 52 (5), 861–870. doi:10.1007/s00254-006-0528-2

Gałuszka, A., Migaszewski, Z. M., and Zalasiewicz, J. (2013). Assessing the anthropocene with geochemical methods. *Geol. Soc. Lond. Spec. Publ.* 395 (1), 221–238. doi:10.1144/sp395.5

Gałuszka, A., Migaszewski, Z. M., Dołęgowska, S., Michalik, A., and Duczmal-Czernikiewicz, A. (2015). Geochemical background of potentially toxic trace elements in soils of the historic copper mining area: a case study from Miedzianka Mt., Holy Cross Mountains, south-central Poland. *Environ. Earth Sci.* 74 (6), 4589–4605. doi:10.1007/s12665-015-4395-6

Garrett, R. G. (2019). *Why minus 80 mesh? Explore*. News Letter of the Association of Applied Geochemists, 1–10.

Grunsky, E. C. (2010). The interpretation of geochemical survey data. *Geochem. Explor. Environ. Anal.* 10 (1), 27–74. doi:10.1144/1467-7873/09-210

Grunsky, E. C., and Caritat, P. D. (2020). State-of-the-art analysis of geochemical data for mineral exploration. *Geochem. Explor. Environ. Anal.* 20 (2), 217–232. doi:10.1144/geochem2019-031

Grunsky, E. C., and de Caritat, P. (2017). Advances in the use of geochemical data for mineral exploration. *Proc. Explor.* 17, 441–456.

Jean-Lavenir, N. M., Cyrille, S., Omar, E. D., Yiika, L. P., and Junior, E. E. M. (2025). Geochemical and gold-ore potential assessment in stream sediments of Bindiba gold District, Eastern Cameroon: implications for gold exploration, sediment provenance, paleoenvironment, and tectonic setting. *Min. Metallurgy Explor.* 42, 2415–2439. doi:10.1007/s42461-025-01270-9

João Pinheiro, F. (2019). *Produto interno bruto dos municípios de Minas Gerais: Ano de referência 2017*. FJP: Belo Horizonte.

Kaiser, H. F. (1958). The varimax criterion for analytic rotation in factor analysis. *Psychometrika* 23 (3), 187–200. doi:10.1007/bf02289233

Klein, C., and Dutrow, B. (2007). *Manual of mineral science*. John Wiley and Sons.

Lapworth, D. J., Knights, K. V., Key, R. M., Johnson, C. C., Ayoade, E., Adekanmi, M. A., et al. (2012). Geochemical mapping using stream sediments in west-central Nigeria: implications for environmental studies and mineral exploration in West Africa. *Appl. Geochem.* 27 (6), 1035–1052. doi:10.1016/j.apgeochem.2012.02.023

Licht, O. A. B. (2020). Geochemical background - what a complex meaning has such a simple expression. *Geochim. Bras.* 34 (2), 161–175. doi:10.21715/gb2358-2812.2020342161

Liu, Y., Cheng, Q., Zhou, K., Xia, Q., and Wang, X. (2016). Multivariate analysis for geochemical process identification using stream sediment geochemical data: a perspective from compositional data. *Geochem. J.* 50 (4), 293–314. doi:10.2343/geochemj.2.0415

Marques, E. D., Castro, C. C., de Assis Barros, R., Lombello, J. C., de Souza Marinho, M., Araujo, J. C. S., et al. (2023). Geochemical mapping by stream sediments of the NW portion of Quadrilátero Ferrífero, Brazil: application of the exploratory data analysis (EDA) and a proposal for generation of new gold targets in Pitangui gold district. *J. Geochem. Explor.* 250, 107232. doi:10.1016/j.gexplo.2023.107232

Matschullat, J., Ottenstein, R., and Reimann, C. (2000). Geochemical background - can we calculate it? *Environ. Geol.* 39 (9), 990–1000. doi:10.1007/s002549900084

Medeiros Filho, L. C., Salomão, G. N., Dall'Agnol, R., de Almeida, G. S., Amarante, R. T., Sahoo, P. K., et al. (2025). Spatial distribution, potential sources and geochemical baseline of Fe and potentially toxic elements in stream sediments in Quadrilátero Ferrífero, Brazil. *Appl. Geochem.*, 106483.

Meloni, F., Dinelli, E., Cabassi, J., Nisi, B., Montegrossi, G., Rappuoli, D., et al. (2025). Provenance and distribution of potentially toxic elements (PTEs) in stream sediments from the eastern Hg-district of Mt. Amiata (central Italy). *Environ. Geochem. Health* 47 (4), 123. doi:10.1007/s10653-025-02434-8

Monteiro, L. V. S. (2002). *Modelamento metalogenético dos depósitos de zinco de Vazante, Fagundes e Ambrósia, associados ao Grupo Vazante, Minas Gerais*. São Paulo: Universidade de São Paulo. [dissertation]. doi:10.11606/t.44.2002.tde-08062013-111126

Moreira, D. S. (2015). "Estratigrafia, Petrografia e Gênese da mineralização de Potássio em Siltitos Verdes (Verdetes) do Grupo Bambuí na região de São Gotardo, Minas Gerais," in *Belo Horizonte: universidade Federal de Minas Gerais*. [dissertation].

Niu, S., Wang, R., and Jiang, Y. (2024). Quantification of heavy metal contamination and source in urban water sediments using a statistically determined geochemical baseline. *Environ. Res.* 263, 120080. doi:10.1016/j.envres.2024.120080

Pereira, R. S., and Fuck, R. A. (2005). Archean nucleii and the distribution of kimberlite and related rocks in the São Francisco craton, Brazil. *Rev. Bras. Geociências* 35 (3), 297–310.

Petrik, A., Jordan, G., Albanese, S., Lima, A., Rolandi, R., and De Vivo, B. (2017). Spatial pattern analysis of Ni concentration in topsoils in the Campania Region (Italy). *J. Geochem. Explor.* 195, 130–142. doi:10.1016/j.gexplo.2017.09.009

Pinho, J. M. M., Féboli, W. L., Signorelli, N., Tuller, M. P., Brito, D. C., Ribeiro, J. H., et al. (2017). *Geologia e recursos minerais das folhas: Cabeceira Grande, Unaí, Ribeirão Arrojado, Serra da Aldeia, Serra da Tiririca, Paracatu, Guarda-Mor, Arrenegado, Coromandel, Lagamar, Monte Carmelo e Patos de Minas*. Belo Horizonte: CPRM.

Rawlins, B. G. (2011). Controls on the phosphorus content of fine stream bed sediments in agricultural headwater catchments at the landscape-scale. *Agric. Ecosyst. Environ.* 144 (1), 352–363. doi:10.1016/j.agee.2011.10.002

Reimann, C., and De Caritat, P. (2005). Distinguishing between natural and anthropogenic sources for elements in the environment: regional geochemical surveys versus enrichment factors. *Sci. Total Environ.* 337 (1–3), 91–107. doi:10.1016/j.scitotenv.2004.06.011

Reimann, C., and De Caritat, P. (2017). Establishing geochemical background variation and threshold values for 59 elements in Australian surface soil. *Sci. Total Environ.* 578, 633–648. doi:10.1016/j.scitotenv.2016.11.010

Reimann, C., Filzmoser, P., and Garrett, R. G. (2002). Factor analysis applied to regional geochemical data: problems and possibilities. *Appl. Geochem.* 17 (3), 185–206. doi:10.1016/s0883-2927(01)00066-x

Reimann, C., Filzmoser, P., Garrett, R. G., and Dutter, R. (2008). *Statistical data analysis explained*. Chichester: John Wiley and Sons, Ltd.

Ribeiro, M. L., Lourencetti, C., Pereira, S. Y., and De Marchi, M. R. R. (2007). Contaminação de águas subterrâneas por pesticidas: avaliação preliminar. *Quím. Nova* 30 (3), 688–694. doi:10.1590/s0100-40422007000300031

Rose, A. W., Hawkes, H. E., and Webb, J. S. (1979). In: *Geochemistry in mineral exploration*. Academic Press, London.

Rudnick, R. L., and Gao, S. (2003). "Composition of the continental crust," in *Treatise on geochemistry, volume 3:* the crust. Editor R. L. Rudnick (Oxford: Elsevier-Pergamon), 1–64.

Saadati, H., Afzal, P., Torshizian, H., and Solgi, A. (2020). Geochemical exploration for lithium in NE Iran using the geochemical mapping prospectivity index, staged factor analysis, and a fractal model. *Geochem. Explor. Environ. Anal.* 20 (4), 461–472. doi:10.1144/geochem2020-020

Sahoo, P. K., Dall'Agnol, R., Salomão, G. N., Ferreira, J. S., Silva, M. S., Jr., Martins, G. C., et al. (2020). Source and background threshold values of potentially toxic elements in soils by multivariate statistics and GIS-based mapping: a high density sampling survey in the Parauapebas basin, Brazilian Amazon. *Environ. Geochem. Health* 42 (1), 255–282. doi:10.1007/s10653-019-00345-z

Sahoo, P. K., Dall'Agnol, R., Salomão, G. N., Ferreira, J. S., Silva, M. S., Jr., Souza, P. W. M. E., et al. (2020). Regional-scale mapping for determining geochemical background values in soils of the Itacaiúnas River Basin, Brazil: the use of compositional data analysis (CoDA). *Geoderma*, 376, 114504. doi:10.1016/j.geoderma.2020.114504

Salomão, G. N. (2020). "Mapeamento geoquímico da bacia do rio Itacaiúnas, Província Mineral de Carajás: Assinatura geoquímica dos blocos crustais e implicações para recursos minerais e meio ambiente," in *Belém: universidade Federal do Pará*. [dissertation].

Salomão, G. N., Figueiredo, M. A., Dall'Agnol, R., Sahoo, P. K., De Medeiros Filho, C. A., Da Costa, M. F., et al. (2019). Geochemical mapping and background concentrations of iron and potentially toxic elements in active stream sediments from Carajás, Brazil – implication for risk assessment. *J. S. Am. Earth Sci.* 92, 151–166. doi:10.1016/j.jsames.2019.03.014

Salomão, G. N., Farias, D. D. L., Sahoo, P. K., Dall'Agnol, R., and Sarkar, D. (2021). Integrated geochemical assessment of soils and stream sediments to evaluate source-sink relationships and background variations in the Parauapebas River Basin, Eastern Amazon. *Soil Syst.* 5 (1), 21. doi:10.3390/soilsystems5010021

Sanford, R. F., Pierson, C. T., and Crovelli, R. A. (1993). An objective replacement method for censored geochemical data. *Math. Geol.* 25 (1), 59–80. doi:10.1007/bf00890676

Silva, M. A., Pinto, C. P., Pinheiro, M. A. P., Marinho, M. S., Lombello, J. C., Pinho, J. M. M. P., et al. (2020). "Mapa Geológico do Estado de Minas Gerais," in Projeto Geologia do Estado de Minas Gerais. *Escala 1:1.000.000*. Belo Horizonte.

Silva-Filho, E. V., Marques, E. D., Vilaça, M., Gomes, O. V., Sanders, C. J., and Kutter, V. T. (2014). Distribution of trace metals in stream sediments along the Trans-Amazonian Federal Highway, Pará State, Brazil. *J. S. Am. Earth Sci.* 54, 182–195. doi:10.1016/j.jsames.2014.04.011

Slezak, P. R., Olivo, G. R., Oliveira, G. D., and Dardenne, M. A. (2013). Geology, mineralogy, and geochemistry of the Vazante Northern extension zinc silicate deposit, Minas Gerais, Brazil. *Ore Geol. Rev.* 56, 234–257. doi:10.1016/j.oregeorev.2013.06.014

Souza, C. M., Shimbo, J. Z., Rosa, M. R., Parente, L. L., Alencar, A. A., Rudorff, B. F. T., et al. (2020). Reconstructing three decades of land use and land cover changes in Brazilian biomes with Landsat archive and Earth engine. *Remote Sens.* 12 (17), 2735. doi:10.3390/rs12172735

Spearman, C. (1904). The proof and measurement of association between two things. *Am. J. Psychol.* 15 (1), 72–101. doi:10.2307/1412159

Steegen, A., Govers, G., Takken, I., Nachtergaele, J., Poesen, J., and Merckx, R. (2001). Factors controlling sediment and phosphorus export from two Belgian agricultural catchments. *J. Environ. Qual.* 30 (4), 1249–1258. doi:10.2134/jeq2001.3041249x

Talebi, H., Mueller, U., Tolosana-Delgado, R., and Van Den Boogaart, K. G. (2018). Geostatistical simulation of geochemical compositions in the presence of multiple geological units: application to mineral resource evaluation. *Math. Geosci.* 51 (2), 129–153. doi:10.1007/s11004-018-9763-9

Thornton, I., Farago, M. E., Thums, C. R., Parrish, R. R., McGill, R. A., Breward, N., et al. (2008). Urban geochemistry: research strategies to assist risk assessment and remediation of brownfield sites in urban areas. *Environ. Geochem. Health* 30 (6), 565–576. doi:10.1007/s10653-008-9182-9

Uhlein, A., Fonseca, M. A., Seer, H. J., and Dardenne, M. A. (2012). Tectônica da faixa de dobramentos Brasília – setores setentrional e meridional. *Rev. Geonomos* 2 (20). doi:10.18285/geonomos.v2i20.243

Vilor, N. V., Kaz'min, L. A., and Pavlova, L. A. (2014). Aresenopyrite-pyrite paragenesis in gold deposits (thermodynamic modeling). *Russ. Geol. Geophys.* 55 (7), 824–841. doi:10.1016/j.rgg.2014.06.003

Yang, Y. G., He, Z. L., Lin, Y., and Stoffella, P. J. (2010). Phosphorus availability in sediments from a tidal river receiving runoff water from agricultural fields. *Agric. Water Manag.* 97 (11), 1722–1730. doi:10.1016/j.agwat.2010.06.003

Yariv, S., and Cross, H. (1979). "Colloid geochemistry of clay minerals," in *Geochemistry of modern sediments*. Editor E. M. Lerman (Berlin, Heidelberg: Springer), 287–333. doi:10.1007/978-3-642-67041-1_8

Yariv, S., and Cross, H. (2001). *Organo-clay complexes and interactions*. Boca Raton, FL: CRC Press. doi:10.1201/9781482270945